Journal of Nuclear Medicine, published on December 4, 2014 as doi:10.2967/jnumed.114.144840

^{89}Zr-bevacizumab PET Visualizes Heterogeneous Tracer Accumulation in Tumor Lesions of Renal Cell Carcinoma Patients and Differential Effects of Anti-angiogenic Treatment

Sjoukje F. Oosting[1], Adrienne H. Brouwers[2], Suzanne C. van Es[1], Wouter B. Nagengast[3], Thijs H. Oude Munnink[1], Marjolijn N. Lub-de Hooge[2,4], Harry Hollema[5], Johan R. de Jong[2], Igle J. de Jong[6], Sanne de Haas [7], Stefan J. Scherer[8], Wim J. Sluiter[5], Rudi A. Dierckx[2], Alfons H.H. Bongaerts[9], Jourik A. Gietema[1], Elisabeth G.E. de Vries[1]

[1]*Department of Medical Oncology, University of Groningen, University Medical Center Groningen, the Netherlands.*

[2]*Department of Nuclear Medicine and Molecular Imaging, University of Groningen, University Medical Center Groningen, the Netherlands.*

[3]*Department of Gastroenterology and Hepatology, University of Groningen, University Medical Center Groningen, the Netherlands.*

[4]*Department of Hospital and Clinical Pharmacy, University of Groningen, University Medical Center Groningen, the Netherlands.*

[5]*Department of Pathology, University of Groningen, University Medical Center Groningen, the Netherlands.*

[6]*Department of Urology, University of Groningen, University Medical Center Groningen, the Netherlands.*

[7]*F. Hoffmann-La Roche, Basel, Switzerland.*

[8]*Genentech, San Francisco, CA.*

[9]*Department of Radiology, University of Groningen, University Medical Center Groningen, the Netherlands.*

Corresponding author:

Sjoukje F. Oosting, MD PhD

Department of Medical Oncology

University Medical Center Groningen

P.O. Box 30 001

9700 RB Groningen, The Netherlands

Phone (+31)50 3612821

Fax (+31)50 3614862

E-mail: s.oosting@umcg.nl

Word count of text: 4997

Word count of abstract: 290

Funding: Supported by a grant from F. Hoffmann-La Roche.

Running foot line: [89]Zr-bevacizumab PET in RCC patients.

Abstract

No validated predictive biomarkers for anti-angiogenic treatment of metastatic renal cell carcinoma (mRCC) exist. Tumor vascular endothelial growth factor A (VEGF-A) level may be useful. We determined tumor uptake of ^{89}Zr-bevacizumab, a VEGF-A-binding positron-emission-tomography (PET) tracer, in mRCC patients before and during anti-angiogenic treatment in a pilot study.

Methods: Patients underwent ^{89}Zr-bevacizumab PET scans at baseline and 2 and 6 weeks after initiating either bevacizumab 10 mg/kg every 2 weeks with interferon-α 3-9 million IU 3x/week (n = 11), or sunitinib 50 mg daily, 4 of every 6 weeks (n =11). Standardized uptake values (SUV) were compared to plasma VEGF-A and time to disease progression.

Results: ^{89}Zr-bevacizumab PET scans visualized 125 evaluable tumor lesions in 22 patients with a median SUVmax of 6.9 (range 2.3–46.9). Bevacizumab/interferon-α induced a mean change in tumor SUVmax of -47.0% (range -84.7 to +20.0%, $P < 0.0001$) at 2 weeks and an additional -9.7% (range -44.8 to +38.9%, $P = 0.015$) at 6 weeks. In the sunitinib group the mean change in tumor SUVmax was -14.3% at 2 weeks (range -80.4 to +269.9, $P = 0.006$), but at 6 weeks the mean change in tumor SUVmax was +72.6% (range -46.4 to +236%, $P < 0.0001$) above baseline. SUVmax was not related to plasma VEGF-A at all scan moments. Baseline mean tumor SUVmax > 10.0 in the three most intense lesions corresponded with longer time to disease progression (89.7 versus 23.0 weeks, hazard ratio 0.22, 95% CI 0.05–1.00).

Conclusion: Tumor uptake of ^{89}Zr-bevacizumab is high in mRCC with remarkable inter-patient and intra-patient heterogeneity. Bevacizumab/interferon-α strongly decreases tumor uptake whereas sunitinib results in a modest reduction with an overshoot after 2 drug-free weeks. High baseline tumor SUVmax was associated with longer time to progression.

Key words: Renal Cell Carcinoma, Molecular Imaging, Positron Emission Tomography, Bevacizumab, Sunitinib.

INTRODUCTION

Angiogenesis inhibitors have single-agent activity and double median progression-free survival in patients with metastatic renal cell carcinoma (mRCC) (*1-3*). However, not all patients respond, and angiogenesis inhibitors are expensive and can have side effects. Furthermore, studies indicated potential tumor-promoting effects of tyrosine kinase inhibitors (TKIs) (*4,5*). Therefore, it is crucial to develop a predictive biomarker for selecting patients who will benefit from these treatments. Circulating vascular endothelial growth factor A (VEGF-A) levels do not predict benefit from anti-angiogenic treatment (*6-10*). VEGF-A however comprises different splice variants; small isoforms can diffuse freely whereas larger isoforms are primarily matrix bound and have biologic activity in the tumor microenvironment (*11*). Local VEGF-A concentration potentially reflects whether angiogenesis drives tumor progression and might predict sensitivity to anti-angiogenic treatment. Therefore we developed the positron emission tomography (PET) tracer ^{89}Zr-bevacizumab, which enables non-invasive whole body VEGF-A imaging and quantification (*12-14*). Sunitinib and bevacizumab plus interferon-α (IFNα) are standard treatments for mRCC (*1,2*). Bevacizumab, a monoclonal antibody with a half-life of ±20 days, binds VEGF-A, thus preventing the growth factor to activate its receptor. Sunitinib is a small molecule with a half-life of ±2 days that blocks VEGF-receptors and other tyrosine kinases intracellularly .

We conducted a pilot study in mRCC patients. RCC is characterized by Von Hippel-Lindau gene inactivation, resulting in high VEGF-A production and characteristic vascular tumors. The primary aim was to quantify ^{89}Zr-bevacizumab uptake in tumor lesions before treatment and changes in uptake during the early course of anti-angiogenic therapy in mRCC patients. Furthermore, we wanted to explore if ^{89}Zr-bevacizumab PET can early identify primary resistant disease (defined as progressive disease at first evaluation); if tumor ^{89}Zr-

bevacizumab uptake correlates with plasma VEGF-A; and explore the effect of 2 drug-free weeks after 4 weeks of sunitinib on tumor ^{89}Zr-bevacizumab uptake.

MATERIALS AND METHODS

Patients

Adult mRCC patients with measurable disease were eligible. Exclusion criteria included uncontrolled hypertension, known untreated brain metastases, clinically significant cardiovascular disease, surgery and TKI treatment up to 4 weeks or bevacizumab up to 4 months before trial entry. The study was approved by the institutional review board, and all subjects signed written informed consent. The trial is registered with ClinicalTrials.gov (NCT00831857).

Study Design and Treatment

The primary endpoint was change of tumor standardized uptake values (SUV) at 2 and 6 weeks after start of treatment. Patients were randomized to bevacizumab 10 mg/kg intravenously every 14 days with IFNα 3 million IU 3 times/week, which was increased after 2 weeks to 6 and then to 9 million IU when tolerated, or sunitinib 50 mg daily orally during 4 of every 6 weeks. Treatment was continued until disease progression or unacceptable toxicity. After inclusion of three patients the study was amended to a non-randomized design because of slow accrual. As no formal comparison of treatment groups was planned, randomization was not essential for conduct of the study. Secondary endpoint was progressive disease at 3 months according to the response evaluation criteria in solid tumors, version 1.1 (RECIST1.1).

Imaging Techniques

Patients underwent ^{89}Zr-bevacizumab PET imaging at baseline, and 2 and 6 weeks after start of treatment. PET scanning was performed 4 days after intravenous administration of 37 MBq ^{89}Zr-bevazicumab (5 mg protein dose). Two weeks is the minimum interval required to avoid interference of activity of the first ^{89}Zr-bevacizumab injection. Six weeks was chosen to explore a rebound phenomenon after 2 sunitinib free weeks, and to explore if a scan after 3 therapeutic bevacizumab doses shows a further change. Conjugation and labeling were done as described earlier (*13*). Patients were scanned from upper thigh to head in up to eight consecutive bed positions with a final reconstruction resolution of ~11 mm. Patients underwent routine computed tomography (CT) imaging at baseline and every 3 months thereafter. CT was performed with intravenous contrast with a maximal slice thickness of 5.0 mm (see Supplemental Methods). In case of symptoms, bone scintigraphy and magnetic resonance imaging (MRI) were performed.

Imaging Data Analysis

Baseline PET scans were qualitatively assessed by a nuclear medicine physician and fused with the baseline CT scans to verify location and anatomic substrate of hot spots. All regions with high focal tracer uptake relative to normal organ background were considered as lesions. Lesions were defined evaluable when identified as tumor lesion on routine imaging, > 10 voxels, delineable from normal organ background, and not irradiated. Quantification was performed with AMIDE Medical Image Data Examiner software (version 0.9.1, Stanford University) (*15*). Maximum and mean SUV were calculated for evaluable lesions and normal organs. All lesions on the baseline CT were measured for comparison with PET. Treatment response was assessed according to RECIST1.1 by a radiologist who was blinded to patient characteristics and PET results.

Biomarker Analysis

Plasma VEGF-A was measured in samples drawn at day -3, day 11 and day 39 before tracer administration and stored at –80˚C until analysis. Samples were analyzed with immunologic multi-parametric chip technique (*7*).

Statistical Assessments

We assumed that the difference in SUV between the baseline scan and the scan after 2 and 6 weeks is ≥ 1.25 standard deviation and that there is no correlation between the first and second scan and estimated that 11 patients were required in each treatment group to predict with 80% power (two-sided $\alpha = 0.05$) that there is a true difference. To compensate for an anticipated 15% early discontinuation, 26 patients were included. For comparison of paired and non-paired data, Wilcoxon's paired rank and the Mann Whitney test were used. Association between SUVmean and SUVmax was analyzed with Spearman's rank correlation, between imaging results and time to disease progression (TTP) with the Kaplan Meier method. Analyses were performed with SPSS version 20 (IBM).

RESULTS

Patients

Between February 2009 and July 2011, 26 patients were included. Two patients did not meet eligibility criteria because of recent bevacizumab treatment and were excluded from the analysis. One patient was not evaluable and one patient withdrew consent. Therefore 22 patients, 11 per treatment group, who underwent at least the baseline and 2-week scan, were evaluable (see Supplemental Fig.1). One patient reported nausea, redness of the face and cold extremities for 24 hours after the third tracer injection, but continued bevacizumab treatment without adverse events. Patient characteristics are shown in Table 1.

Baseline ^{89}Zr-bevacizumab PET

Normal Organ ^{89}Zr-Bevacizumab Uptake. An example of a baseline scan is shown in Fig. 1. SUVmean and SUVmax of normal organs were strongly correlated ($r^2 = 0.99$, $P < 0.0001$, Supplemental Fig. 2A). SUVmax is less operator-dependent, so we used SUVmax. Normal organ uptake (Fig. 2A) was consistent with a previous study (*14*) as well as with distribution of other antibody tracers (*16,17*).

Tumor ^{89}Zr-Bevacizumab Uptake. ^{89}Zr-bevacizumab PET visualized lesions in all patients. In total, 213 lesions were identified, of which 194 were in the field of view of the routine CT scan; 159 were also identified as tumor lesions on CT. The 35 lesions that were not detected on CT were located in the bone ($n = 12$), lymph nodes ($n = 6$), muscles ($n = 7$), kidneys ($n = 4$), intra-peritoneal ($n = 4$) and retroperitoneal compartment ($n = 2$). The 19 lesions outside the field of view of the CT were localized in the brain ($n = 5$ in 3 patients), bone ($n = 4$), lymph nodes ($n = 2$) and muscles ($n = 8$) (Table 2). Two patients with known brain metastases had radiotherapy before entry in the study. In the third patient no MRI was performed. Sunitinib was started immediately because of rapidly progressive systemic disease without neurological symptoms. On CT 562 lesions were identified, 145 in the bevacizumab/IFNα group and 412 in the sunitinib group, of which 231 were ≥ 10 mm. The smallest lesion detected by ^{89}Zr-bevacizumab PET was 5.0 mm. The detection percentage increased with lesion size on CT (Supplemental Fig. 3); 56.7% of lesions ≥ 10 mm were visible with ^{89}Zr-bevacizumab PET. The 125 tumor lesions evaluable for quantification showed a strong correlation between SUVmean and SUVmax ($r^2 = 0.99$, $P < 0.0001$, Supplemental Fig. 2B). Therefore only SUVmax is reported. Median tumor SUVmax was 6.9 (range 2.3–46.9), varying from 3.8 (range 2.7–15.4) for the patient with the lowest tumor uptake to 36.3 (range 25.7–46.9) for the patient with the highest uptake (Fig. 2B). Furthermore, tumor tracer uptake differed according to organ localization (Fig. 2C).

Serial ^{89}Zr-Bevacizumab PET Before And During Bevacizumab/IFNα

At baseline, median SUVmax in 34 tumor lesions in the bevacizumab/IFNα treated patients was 8.1 (range 2.3–46.9). At 2 weeks, a mean change of -47.0% in tumor SUVmax (range -84.7 to +20.0%, $P < 0.0001$) was found, resulting in a median SUVmax of 4.7 (range 1.4–10.1; Fig. 3A). This pattern was found in all patients (Supplemental Fig. 4A). Tumor SUVmax consistently decreased to ≤ 10, even in lesions with very high baseline uptake (Fig. 3B). A third ^{89}Zr-bevacizumab PET scan, available in nine patients, showed a further mean change of -9.7% (range -44.8 to +38.9%, $P = 0.015$) in tracer uptake in the 23 tumor lesions (Fig. 3A). Fig. 4A shows an example of serial scans. Small changes over time in normal organ ^{89}Zr-bevacizumab uptake were detected (Supplemental Fig. 5A).

Serial ^{89}Zr-Bevacizumab PET Before And During Sunitinib

Median SUVmax in 91 tumor lesions in patients receiving sunitinib was 6.7 at baseline (range 2.4–34.2). After 2 weeks of treatment, a mean change in tumor SUVmax of -14.3% was found (range -80.4 to +269.9, $P = 0.006$), with a median SUVmax of 4.3 (range 0.7–83.8) at 2 weeks (Fig. 3C and D). At the patient level, patterns were divergent (Supplemental Fig. 4B). Mean change in tumor SUVmax differed according to organ site: in kidney ($n = 7$) a mean increase of 66.2% (range -19.4 to +201.8%) was found whereas in lung ($n = 36$) and lymph node metastases ($n = 24$) SUVmax decreased: -52.3% (range -80.4 to +8.2%, $P < 0.0001$) and -26.0% (range -65.2 to +26.2%, $P = 0.002$) respectively. A third ^{89}Zr-bevacizumab PET scan in six patients showed 42 evaluable lesions. A mean increase of 89.3% (range -37.2 to +411%, $P = 0.0001$) in tumor SUVmax was found after 2 sunitinib-free weeks corresponding to a mean increase of 72.6% above baseline (range -46.4 to +236.0%, $P < 0.0001$, Fig. 3C). Fig. 4B shows an example of serial scans. Normal liver, kidney and spleen uptake increased during sunitinib by 51.1%, 32.7% and 25.0% respectively, and returned to baseline after 2 drug-free

weeks. In other normal organs, mean absolute changes did not exceed 1.0 SUVmax (Supplemental Fig. 5B).

^{89}Zr-Bevacizumab PET And Treatment Outcome

Eighteen patients were evaluable for tumor response at 3 months (Table 3). One patient with a sarcomatoid tumor component on bevacizumab/IFNα had progressive disease, one patient had a partial response and 16 patients had stable disease. The patient with progressive disease had a mean baseline tumor SUVmax of 6.4 which had decreased by 34% at 2 weeks. Posthoc analysis showed that 16 patients (eight of both treatment groups) with a baseline tumor SUVmax > 10.0 in the three most intense lesions had a longer TTP compared to six patients (three of both treatment groups) with lower baseline tumor SUVmax, with a median TTP of 89.7 compared to 23.0 weeks (hazard ratio 0.22, 95% confidence interval 0.05–1.00, $P = 0.050$; Fig. 5). A cut off of 10 was chosen because mean normal organ SUVmax is < 10 and bevacizumab treatment reduced tumor uptake to < 10. Change in tumor uptake and TTP did not correlate.

Plasma VEGF-A

Baseline plasma VEGF-A ($n = 20$, median 101.2 pg/mL, range 15.4–445.1) did not correlate with tumor SUVmax, mean tumor SUVmax of all evaluable lesions and of the three most intense lesions. Plasma VEGF-A during bevacizumab treatment is unreliable and therefore not analyzed. In the sunitinib group, no relationship was found between plasma VEGF-A and tumor SUVmax, mean tumor SUVmax of all evaluable lesions and of the three most intense lesions at 2 and 6 weeks. Also, changes in plasma VEGF-A did not correspond with changes in tumor SUVmax parameters.

DISCUSSION

This pilot study in 22 mRCC patients demonstrates that ^{89}Zr-bevacizumab PET visualizes tumor lesions, with major differences in tumor ^{89}Zr-bevacizumab uptake both between and within patients. Anti-angiogenic therapy alters tumor ^{89}Zr-bevacizumab uptake; a consistent large decrease occurs after start of bevacizumab/IFNα and a heterogeneous response during sunitinib.

There was a striking heterogeneity in ^{89}Zr-bevacizumab tumor accumulation at baseline. In a subset of tumors, uptake did not exceed normal organ background, reflected by visualization of only 56.7% of tumor lesions ≥ 10 mm. Moreover, in evaluable lesions, large differences in SUVmax were found, which may indicate a difference in biology. Tracer accumulation is dependent on delivery by tumor vasculature and on the amount of target. Heterogeneity may therefore reflect differences in vascular characteristics and tumor VEGF-A production. We did not perform biopsies in the current study. However, a correlation between ^{111}In-bevacizumab tumor uptake and VEGF-A expression in melanoma lesions and between ^{89}Zr-bevacizumab tumor uptake and VEGF-A expression in primary breast cancer has been shown previously (*13, 18*).

Inter-patient tumor heterogeneity is increasingly recognized and used for personalized treatment. The heterogeneity of ^{89}Zr-bevacizumab tumor uptake between patients may offer a possibility to differentiate patient groups based on tumor biology. Intra-patient tumor heterogeneity has also drawn increasing attention (*19,20*). Exome sequencing of different parts of primary RCCs and associated metastatic sites demonstrated substantial mutational heterogeneity (*19*). PET imaging has the potential to non-invasively visualize and quantify effects of mutations on expression of treatment targets across tumor lesions (*21)*. Whole body insight in heterogeneity of tumor characteristics might guide choices of drug combinations or combinations of different treatment modalities in the future.

Formal comparison of treatment groups was not the aim of this pilot study. Nevertheless, the finding of increased ^{89}Zr-bevacizumab tumor accumulation at 2 weeks in a subset of lesions during sunitinib suggests a difference in biological effect of the two anti-angiogenic regimens, probably related to the different mechanisms of action. Unlike bevacizumab, sunitinib induces a systemic VEGF release that maybe partly tumor derived (*22, 23*)

Our finding that therapeutic bevacizumab/IFNα reduced ^{89}Zr-bevacizumab tumor delivery may be explained by competition between cold and labeled antibody. However, results of preclinical and clinical studies suggest that bevacizumab induced vascular changes are responsible (*24-26*). Two studies in mice bearing human epidermal growth factor receptor-2 (HER2) expressing tumors, demonstrated that VEGF-A antibody treatment reduced tumor accumulation of the HER2 antibody trastuzumab and a non-specific antibody, while normal tissue distribution was not altered (*24,25*). Decreased tumor accumulation was accompanied by reduced tumor vascular density and blood flow, and increased pericyte coverage of tumor vessels. Furthermore, in non-small cell lung cancer patients, tumor delivery of docetaxel diminished after one therapeutic bevacizumab dose, which was paralleled by reduced tumor perfusion (*26*).

The small decrease that we observed in mean tumor ^{89}Zr-bevacizumab uptake after 2 weeks sunitinib, and the rebound exceeding baseline after 2 weeks off treatment, correspond with our preclinical findings (*27*). Preclinical studies showed increased invasiveness and metastasis following a short sunitinib course (*4,5*). Moreover, a profound expansion of proliferating endothelial cells was demonstrated in primary RCCs after neo-adjuvant sunitinib (*28*). This was not observed after bevacizumab, despite similar histological features suggestive of vascular normalization (*28*). These findings support our observation of different tumor biology after sunitinib and bevacizumab/IFNα. Interestingly, the increased uptake in renal

tumors during sunitinib treatment differs from results of ^{111}In-bevacizumab SPECT in seven RCC patients treated with the TKI sorafenib for 4 weeks (*29*). Reduced tumor ^{111}In-bevacizumab uptake correlated with areas of necrosis (*29*). The increase in ^{89}Zr-bevacizumab accumulation in the normal liver, spleen and kidney during sunitinib treatment is probably due to sunitinib induced release of VEGF-A by normal cells. This was also suggested by the observation of elevated VEGF protein in liver, spleen and kidney tissue of sunitinib treated mice (*5*).

Baseline tumor ^{89}Zr-bevacizumab uptake in our study was higher than in patients with early breast cancer and with metastatic neuroendocrine tumors (*13,14*). This observation probably reflects the unique pathobiology of Von Hippel-Lindau gene inactivation in RCC, resulting in high VEGF-A production by tumor cells.

We had only one patient with progressive disease at 3 months, and therefore no conclusions can be drawn about the ability of ^{89}Zr-bevacizumab PET to identify primary resistant patients. Patients with intense ^{89}Z-bevacizumab tumor accumulation at baseline had a longer TTP. This exploratory analysis should be interpreted with caution, but may indicate that those tumors are more VEGF driven and dependent and therefore can be effectively controlled with anti-angiogenic treatment.

Absence of a correlation between SUVmax parameters and plasma VEGF-A might be due to different composition of circulating and microenvironmental VEGF-A isoforms.

CONCLUSION

We demonstrated heterogeneous ^{89}Zr-bevacizumab tumor uptake in mRCC patients. Bevacizumab/IFNα strongly decreases ^{89}Zr-bevacizumab tumor uptake whereas sunitinib results in modest reduction with an overshoot after 2 drug-free weeks. High baseline tumor SUVmax appears to be associated with longer TTP. Further studies are required to determine if

baseline ^{89}Zr-bevacizumab tumor uptake can be used to predict benefit from anti-angiogenic treatment. To differentiate between prognostic and predictive value, a randomized study is required.

ACKNOWLEDGMENTS

This research was supported by a grant from F. Hoffmann-La Roche to the University Medical Center Groningen.

DISCLOSURE

Conflicts of interest, including specific financial interests and relationships and affiliations relevant to the subject matter or materials discussed in the manuscript are the following: S. de Haas is employee of Roche. S.J. Scherer is former employee of Genentech. J.A. Gietema and E.G.E. de Vries had research grants of Roche which were made available to the UMCG. E.G.E. de Vries served as an advisory board member of Roche-Genentech. No potential conflicts of interest were disclosed by the other authors.

REFERENCES

1. Motzer RJ, Hutson TE, Tomczak P, et al. Sunitinib versus interferon alfa in metastatic renal-cell carcinoma. *N Engl J Med*. 2007;356:115–124.
2. Escudier B, Pluzanska A, Koralewski P, et al. Bevacizumab plus interferon alfa-2a for treatment of metastatic renal cell carcinoma: a randomised, double-blind phase III trial. *Lancet*. 2007;370:2103–2111.
3. Sternberg CN, Davis ID, Mardiak J, et al. Pazopanib in locally advanced or metastatic renal cell carcinoma: results of a randomized phase III trial. *J Clin Oncol*. 2010;28:1061–1068.
4. Pàez-Ribes M, Allen E, Hudock J, et al. Antiangiogenic therapy elicits malignant progression of tumors to increased local invasion and distant metastasis. *Cancer Cell*. 2009;15:220–231.
5. Ebos ML, Lee CR, Cruz-Munoz W, Bjarnason GA, Christensen JG, Kerbel RS. Accelerated metastasis after short-term treatment with a potent inhibitor of tumor angiogenesis. *Cancer Cell*. 2009;15:232–239.
6. Hegde PS, Jubb AM, Chen D, et al. Predictive impact of circulating vascular endothelial growth factor in 4 phase III trials evaluating bevacizumab. *Clin Cancer Res.* 2013;19:929–937.
7. Miles DW, de Haas SL, Dirix LY, et al. Biomarker results from the AVADO phase 3 trial of first-line bevacizumab plus docetaxel for Her2-negative metastatic breast cancer. *Br J Cancer*. 2013;108:1052–1060.
8. Escudier B, Eisen T, Stadler WM, et al. Sorafenib for treatment of renal cell carcinoma: final efficacy and safety results of the phase III treatment approaches in renal cancer global evaluation trial. *J Clin Oncol*. 2009;27:3312–3318.

9. Harmon CS, DePrimo SE, Figlin RA, et al. Circulating proteins as potential biomarkers of sunitinib and interferon-α efficacy in treatment-naïve patients with metastatic renal cell carcinoma. *Cancer Chemother Pharmacol*. 2014;73:151–161.

10. Bais C, Rabe C, Wild N, et al. Comprehensive reassessment of plasma VEGFA (pVEGFA) as a candidate predictive biomarker for bevacizumab (Bv) in 13 pivotal trials (seven indications). *J Clin Oncol.* 2014;32:5s (suppl; abstr 3040)

11. Park JE, Keller GA, Ferrara N. The vascular endothelial growth factor (VEGF) isoforms: differential deposition into the subepithelial extracellular matrix and bioactivity of extracellular matrix-bound VEGF. *Mol Biol Cell.* 1993;4:1317–1326.

12. Nagengast WB, de Vries EG, Hospers GA, et al. In vivo VEGF imaging with radiolabeled bevacizumab in an ovarian tumor xenograft. *J Nucl Med.* 2007;48:1313–1319.

13. Gaykema SBM, Brouwers AH, Lub-de Hooge MN, et al. ^{89}Zr-bevacizumab PET imaging in primary breast cancer. *J Nucl Med*. 2013;54:1014–1018.

14. Van Asselt SA, Oosting SF, Brouwers AH, et al. Everolimus reduces ^{89}Zr-bevacizumab tumor uptake in patients with neuroendocrine tumors. *J Nucl Med.* 2014;55:1087–1092.

15. Loening AM, Gambhir SS. AMIDE: a free software tool for multimodality medical image analysis. *Mol Imaging.* 2003;2:131–137.

16. Dijkers EC, Oude Munnink TH, Kosterink JG, et al. Biodistribution of ^{89}Zr-trastuzumab and PET imaging of HER2-positive lesions in patients with metastatic breast cancer. *Clin Pharmacol Ther*. 2010;87:586–592.

17. Pandit-Taskar N, O'Donoghue JA, Morris MJ, et al. Antibody mass escalation study in patients with castration-resistant prostate cancer using ^{111}In-J591: lesion detectability and dosimetric projections for ^{90}Y radioimmunotherapy. *J Nucl Med*. 2008;49:1066–1074.

18. Nagengast WB, Lub-de Hooge MN, Van Straten EM, et al. VEGF-SPECT with ^{111}In-bevacizumab in stage III/IV melanoma patients. *Eur J Cancer.* 2011;47:1595–1602.

19. Gerlinger M, Rowan AJ, Horswell S, et al. Intratumor heterogeneity and branched evolution revealed by multiregion sequencing. *N Engl J Med*. 2012;366:883–892.

20. Horswell S, Matthews N, Swanton C. Cancer heterogeneity and "The struggle for existence": diagnostic and analytical challenges. *Cancer Lett.* 2013;340:220–226.

21. Petrulli JR, Sullivan JM, Zheng MQ, et al. Quantitative analysis of [11C]-erlotinib PET demonstrates specific binding for activating mutations of the EGFR kinase domain. *Neoplasia.* 2013;15:1347–1353.

22. DePrimo SE, Bello CL, Smeraglia J, et al. Circulating protein biomarkers of pharmacodynamic activity of sunitinib in patients with metastatic renal cell carcinoma: modulation of VEGF and VEGF-related proteins. *J Transl Med*. 2007;5:32.

23. Ebos JM, Lee CR, Christensen JG, Mutsaers AJ, Kerbel RS. Multiple circulating proangiogenic factors induced by sunitinib malate are tumor-independent and correlate with antitumor efficacy. *Proc Natl Acad Sci U S A*. 2007;104:17069–17074.

24. Pastuskovas CV, Mundo EE, Williams SP, et al. Effects of anti-VEGF on pharmacokinetics, biodistribution, and tumor penetration of trastuzumab in a preclinical breast cancer model. *Mol Cancer Ther*. 2012;11:752–762.

25. Arjaans M, Oude Munnink TH, Oosting SF, et al. Bevacizumab-induced normalization of blood vessels in tumors hampers antibody uptake. *Cancer Res*. 2013;73:3347–3355.

26. Van der Veldt AA, Lubberink M, Bahce I, et al. Rapid decrease in delivery of chemotherapy to tumors after anti-VEGF therapy: implications for scheduling of anti-angiogenic drugs. *Cancer Cell*. 2012;21:82–91.

27. Nagengast WB, Lub-de Hooge MN, Oosting SF, et al. VEGF-PET imaging is a non-invasive biomarker showing differential changes in the tumor during sunitinib treatment. *Cancer Res.* 2011;71:143–153.

28. Griffioen AW, Mans LA, de Graaf AM, et al. Rapid angiogenesis onset after discontinuation of sunitinib treatment of renal cell carcinoma patients. *Clin Cancer Res*. 2012;18:3961–3971.

29. Desar IME, Stillebroer AB, Oosterwijk E, et al. ^{111}In-bevacizumab imaging of renal cancer and evaluation of neoadjuvant treatment with the vascular endothelial growth factor receptor inhibitor sorafenib. *J Nucl Med*. 2010;51:1707–1715.

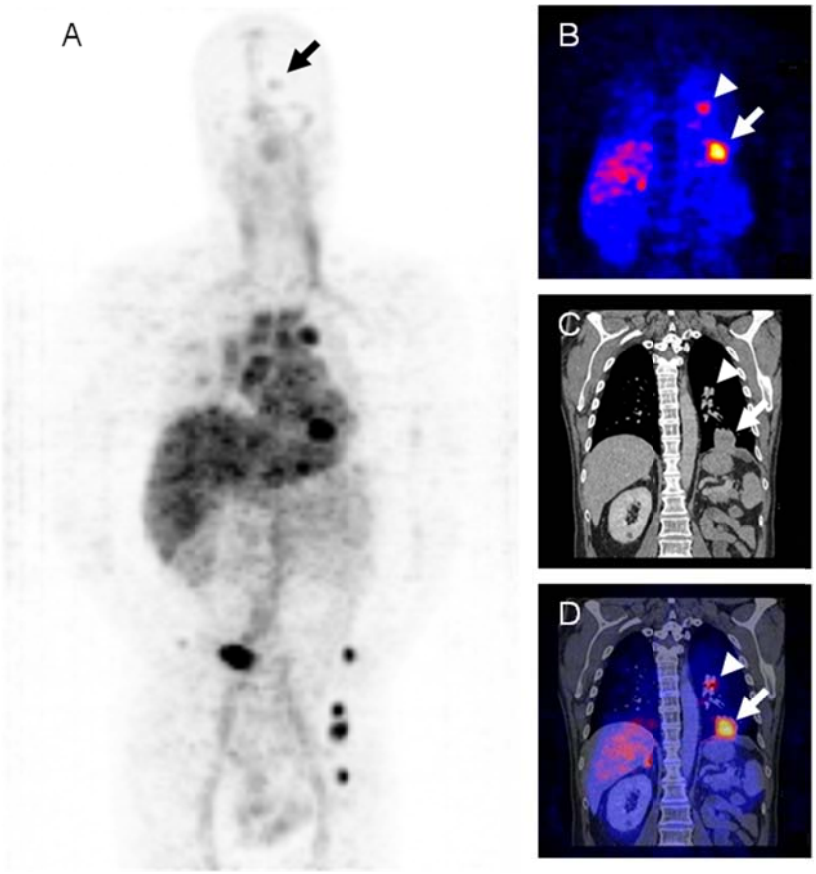

FIGURE 1. (A) Baseline ^{89}Zr-bevacizumab PET scan of a mRCC patient showing tracer in the blood pool, liver, metastases in bone, lung, lymph nodes, and brain (arrow). Coronal ^{89}Zr-bevacizumab PET (B) CT (C) and fusion image (D) of the chest showing lung (large arrow) and lymph node (small arrow) metastases.

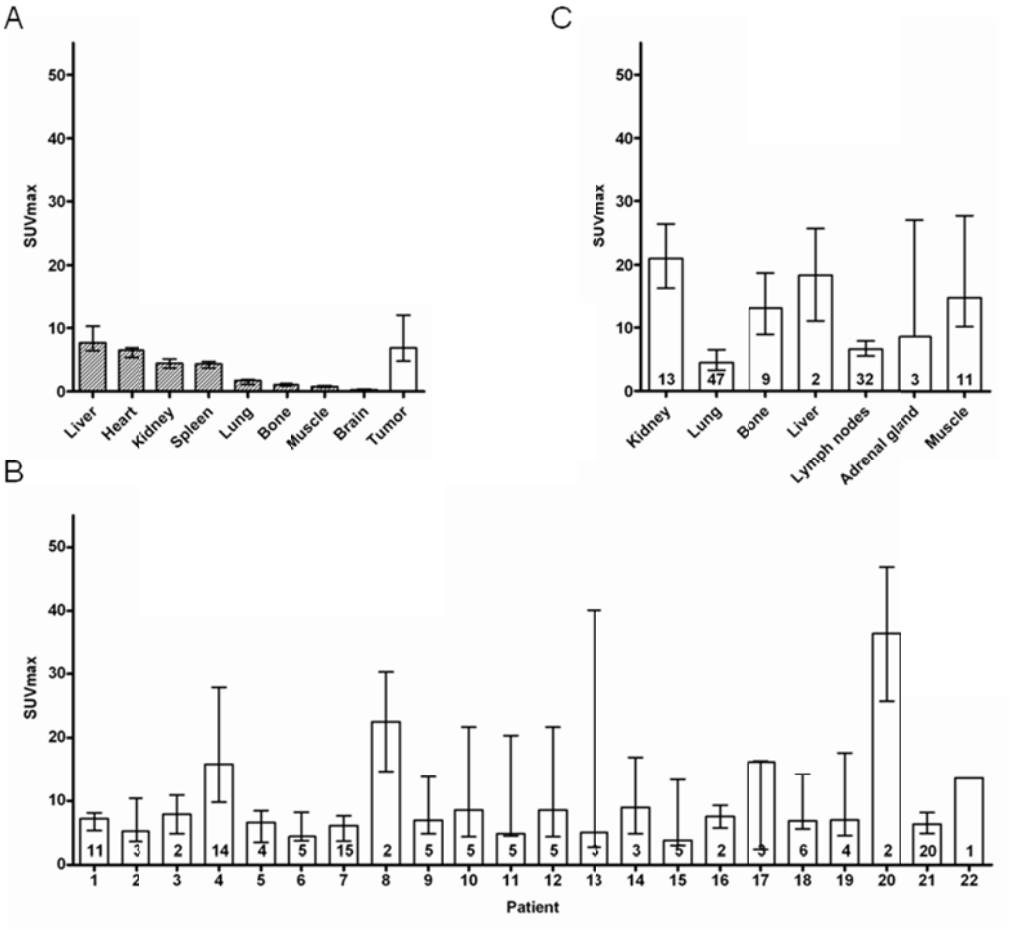

FIGURE 2. (A) Median uptake at baseline in normal organs and all evaluable tumor lesions (*n* = 125) on ^{89}Zr-bevacizumab PET scan with interquartile range. Uptake in tumor lesions per patient (B) and according to organ localization (C), in the bar the number of lesions is indicated.

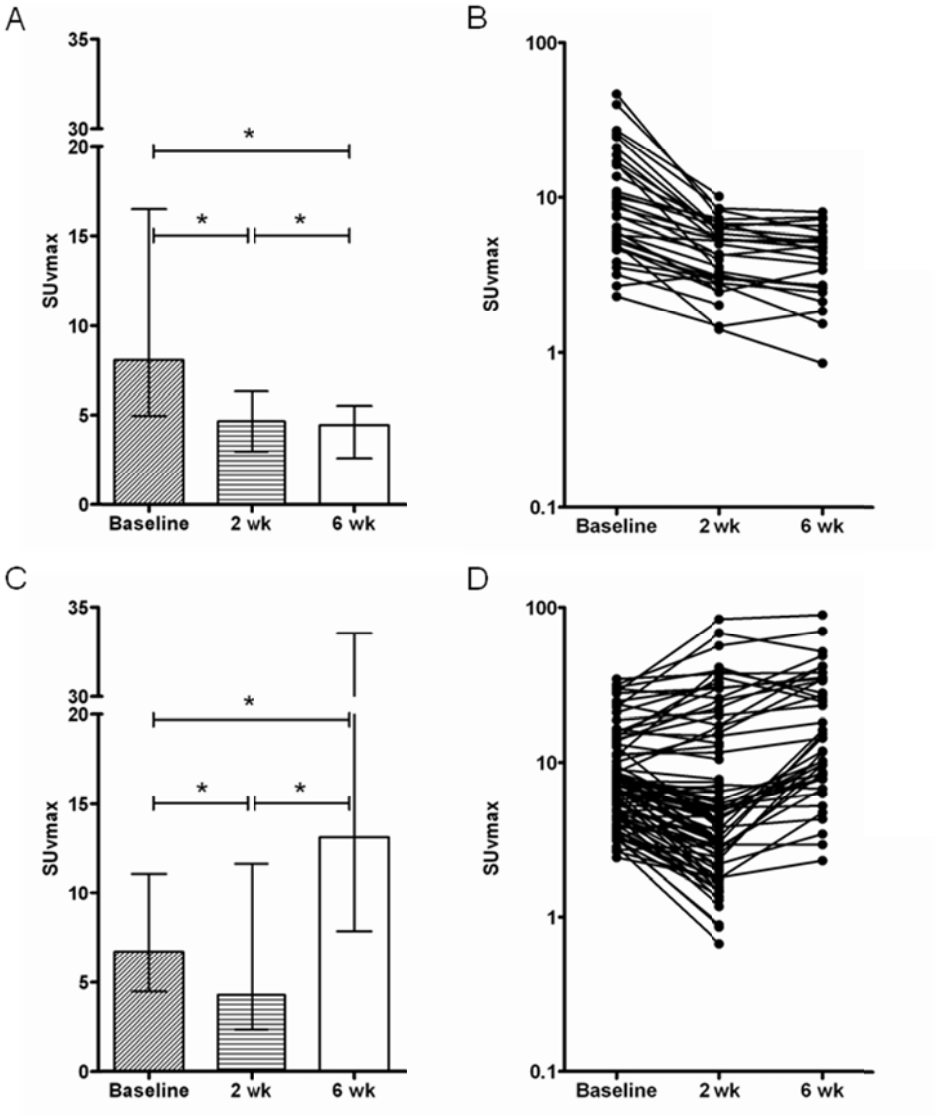

FIGURE 3. ^{89}Zr-bevacizumab tumor uptake before and during anti-angiogenic treatment 11 patients treated with bevacizumab/IFNα (A and B) and in 11 patients treated with sunitinib (C and D). Bars: median SUVmax with interquartile range. Lines: individual tumor lesions. * $P <$ 0.05.

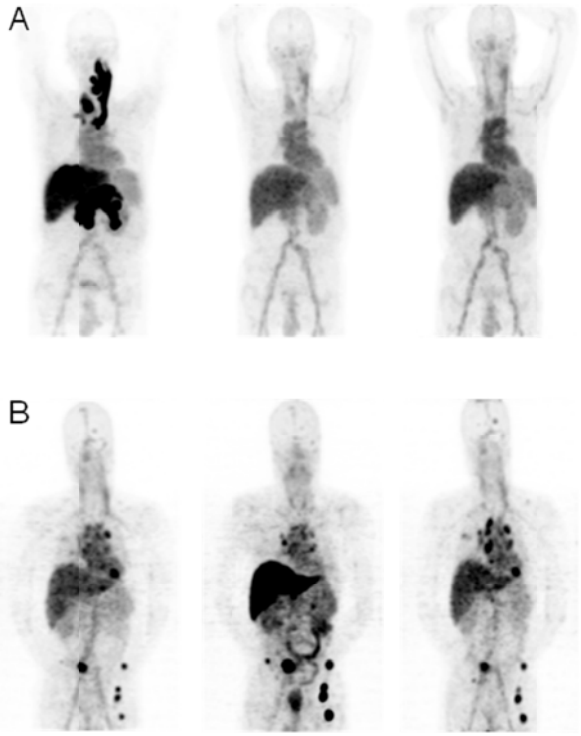

FIGURE 4. (A) Serial ^{89}Zr-bevacizumab PET scans of a patient with RCC metastases in pancreas, liver and thyroid with associated jugular and portal vein thrombosis at baseline (left), and 2 weeks (middle) and 6 weeks (right) after start of bevacizumab/IFNα. Tumor uptake decreases whereas normal organ uptake is stable over time. (B) Serial ^{89}Zr-bevacizumab PET scans of a patient with RCC metastases in the lungs, mediastinal lymph nodes, bone and brain at baseline (left), and 2 weeks (middle) and 6 weeks (right) after start of sunitinib; i.e. after 2 sunitinib-free weeks. Tumor ^{89}Zr-bevacizumab uptake decreases during treatment in lung and brain metastases but increases in normal liver and bone metastases, with the reverse pattern after 2 drug-free weeks.

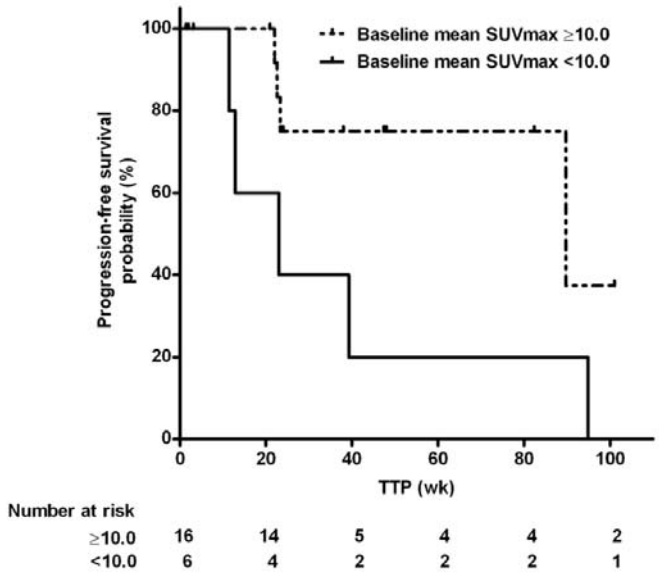

FIGURE 5. Kaplan-Meier analysis of TTP according to baseline ^{89}Zr-bevacizumab tumor uptake of the three most intense tumor lesions. $P = 0.05$.

TABLE 1
Patient demographics and clinical characteristics

Variable	Bevacizumab/ IFNα (*n* = 11)	Sunitinib (*n* = 11)	Total population (*n* = 22)
	n (%)	*n* (%)	*n* (%)
Sex			
Male	7 (64)	11 (100)	18 (82)
Female	4 (36)	0 (0)	4 (18)
Age (years)			
Median	63	57	62
Range	49–74	50–71	49–74
Nephrectomy			
Yes	7 (64)	7 (64)	14 (64)
No	4 (36)	4 (36)	8 (36)
Histology			
Pure clear cell	10 (91)	11 (100)	21 (95)
Mixed	1 (9)	0 (0)	1 (5)
MSKCC criteria			
Good	1 (9)	1 (9)	2 (9)
Intermediate	10 (91)	10 (91)	20 (91)
WHO performance			
0	10 (91)	9 (82)	19 (86)
1	1 (9)	1 (9)	2 (9)
2	0 (0)	1 (9)	1 (5)
Tumor sites			
Kidney	7 (64)	6 (55)	13 (59)
Lung	9 (82)	8 (73)	17 (77)
Lymph node	8 (73)	7 (64)	15 (68)
Bone	3 (27)	6 (55)	9 (41)
Liver	3 (27)	2 (18)	5 (23)
Pancreas	2 (18)	3 (27)	5 (23)
Adrenal	2 (18)	2 (18)	4 (18)
Other	5 (45)	5 (45)	10 (45)
Number of tumor sites			
Median	3	2	3
Range	1–4	2–6	1–6
Previous treatment			
TKI	2 (18)	1 (9)	3 (14)
IFNα	0 (0)	1 (9)	1 (5)
None	9 (82)	8 (73)	16 (73)

MSKCC = Memorial Sloan Kettering Cancer Center, WHO = World Health Organization, TKI = tyrosine kinase inhibitor, INFα = interferon alpha

TABLE 2

Lesions visualized with ^{89}Zr-bevacizumab PET and CT

Organ	PET	CT	Concordant
	n	*n* (*n* ≥ 10 mm)	*n*
Kidney	20	16 (13)	14
Lung	54	391 (93)	54
Bone*	30	15 (11)	14
Liver	3	14 (7)	3
Lymph node*	53	86 (73)	45
Brain*	5	0 (0)	0
Adrenal gland	4	5 (5)	4
Muscle*	29	17 (15)	14
Miscellaneous	15	18 (14)	11
Total	213	562 (231)	159

* Including lesions outside the field of view of the CT scan: bone *n* = 4, lymph node *n* = 2, brain *n* = 5, muscle *n* = 8.

PET = positron emission tomography, CT = computed tomography

TABLE 3

Treatment outcome

Variable	Bevacizumab/ IFNα (*n* = 11)	Sunitinib (*n* = 11)	Total population (*n* = 22)
	n (%)	*n* (%)	*n* (%)
Response at 3 months*			
PR	1 (9)	0 (0)	1 (5)
SD	8 (73)	8 (73)	16 (73)
PD	1 (9)	0 (0)	1 (5)
NE†	1 (9)	3 (27)	4 (18)
Time to progression (weeks)			
Median	23.7	30.8	23.8
Range	11.4–82.4+	12.9–101+	11.4–101+

* According to RECIST1.1.

† 4 patients discontinued treatment because of myocardial infarction (*n* = 2), and hepatotoxicity (*n* = 1) during sunitinib and bowel perforation at a metastatic site (*n* = 1) during bevacizumab/IFNα.

INFα = interferon alpha, PR = partial response, SD = stable disease, PD = progressive disease, NE = not evaluable, + = more than.